J Pharmacol Sci **110**, 285 – 294 (2009)

Journal of Pharmacological Sciences

Full Paper

Polaprezinc (Zinc L-Carnosine) Is a Potent Inducer of Anti-oxidative Stress Enzyme, Heme Oxygenase (HO)-1 — a New Mechanism of Gastric Mucosal Protection

Kazuki Ueda[1], Takashi Ueyama[2,*], Masashi Oka[1], Takao Ito[2], Yoshihiro Tsuruo[2], and Masao Ichinose[1]

[1]*2nd Department of Internal Medicine,* [2]*Department of Anatomy and Cell Biology, Wakayama Medical University, Wakayama 641-8509, Japan*

Received February 17, 2009; Accepted May 7, 2009

Abstract. Heme oxygenase (HO)-1 is implicated in cytoprotection in various organs. We tested a possibility that polaprezinc (PZ), an anti-ulcer drug, could induce HO-1 in the gastric mucosa. Male 6-week-old Wistar rats were intragastrically administered PZ. Gastric expression of HO-1 was assessed by real time RT-PCR and western blotting, and localization of HO-1 was observed by in situ hybridization and immunohistochemistry. The levels of HO-1 mRNA were increased in a dose-dependent manner. The levels of HO-1 mRNA were increased 4-fold by PZ at the dose of 200 mg/kg at 3 h as compared with control levels. The levels of immunoreactive HO-1 were increased 3-fold at 6 h. Signals for HO-1 mRNA and immunoreactivity were detected strongly in the surface gastric mucosal cells and moderately in the gastric macrophages. Treatment with an HO-1 inhibitor, stannous mesoporphyrin (SnMP) significantly worsened the HCl-induced acute gastric mucosal lesions and increased the apoptosis of mucosal cells. Mucosal lesions were decreased by pretreatment with PZ, while they were increased by co-administration with SnMP. These data indicate for the first time that PZ is an effective inducer of HO-1 in the stomach. PZ-induced HO-1 functions as a part of the mucosal protective effects of PZ.

Keywords: heme oxygenase, mucosal protection, zinc compound, apoptosis, gastric mucosa

Introduction

Polaprezinc (PZ), a chelate compound consisting of zinc and L-carnosine, is widely used as an anti-ulcer drug (1). PZ dose-dependently prevents gastric mucosal lesions and mucosal cell damages induced by ethanol (2), monochloramine (3), histamine (4), HCl-aspirin (5), indomethacin (5), water-immersion stress (4), burn shock (6), ischemia–reperfusion (6, 7), *Helicobacter pylori*–associated gastritis (8), duodenal ulcer induced by mepirizole (4), and colitis induced by 2,4,6-trinitrobenzene sulfonic acid (TNB) (9).

Mucosal protection by PZ is attributed to stimulation of mucus production (2), antioxidant activity (6, 7), membrane-stabilizing action (10), and induction of heat shock protein (HSP) 70 (11). Particularly, involvement of HSP families in many pathological conditions including gastric lesions has been extensively studied (12, 13). HSPs are classified into several families according to their apparent molecular weights and respective inducers. Besides HSP70, involvement of HSP32, also regarded as heme oxygenase (HO)-1, in gastrointestinal diseases is reported (14 – 16). HO-1 is the inducible isoform of HO, which catalyzes the first and rate-limiting step in heme degradation to produce equimolar quantities of biliverdin, carbon monoxide (CO), and free iron (17). Biliverdin is subsequently converted to bilirubin via the action of biliverdin reductase, and free iron is promptly sequestered into ferritin. CO and other toxic agents at low concentrations exert distinctly different effects on physiological and cellular functions. CO leads to vasodilation and inhibition of platelet aggregation (18). In addition, bilirubin exhibits the highest endogenous antioxidant activity among the constituents of normal human serum (19). Sequestration of free iron by ferritin lowers the pro-oxidant state of the cell. HO-1–dependent

*Corresponding author. tueyama@wakayama-med.ac.jp
Published online in J-STAGE on June 19, 2009 (in advance)
doi: 10.1254/jphs.09056FP

release of iron also resulted in the up-regulation of ferritin (20). Therefore, induction of HO-1 can provide cytoprotection against oxidative stress.

In this study, we tested the possibility that PZ might induce HO-1 as well as HSP70 in the stomach. Next, we evaluated the effect of PZ-induced HO-1 on the HCl-induced acute mucosal lesions (AGML) and apoptosis of mucosal cells by pretreating them with an HO-1 inhibitor, stannous mesoporphyrin (SnMP) (21).

Materials and Methods

Tissue preparation

Wistar male rats, 5-week-old, were purchased from Kiwa Lab. (Wakayama). Animals were housed in a temperature-controlled environment. Experiments were performed after allowing the rats free access to food and water for one week. The rats were fasted overnight prior to each study in individual wire-bottom cages. PZ (provided by Zeria Pharmaceutical Co., Ltd., Tokyo) was suspended in 0.5% methylcellulose. The rats were administered intra-gastrically (by gastric intubation) PZ at 50, 100, or 200 mg/kg (n = 5, respectively). The rats were decapitated at 3 h after application of PZ. Five fasted rats served as controls. The stomach was rapidly removed, gently rinsed with saline, and several tissue sections were punched out and immediately frozen using powdered dry ice within 1 min after decapitation. The rest of the tissues were fixed in 4% paraformaldehyde in 0.1 M phosphate buffer, pH 7.4 overnight at 4°C, and then cryoprotected in phosphate-buffered saline (PBS) containing 30% sucrose for 3 days at 4°C. The tissue samples were mounted in O.C.T. compound (Tissue-Tek®; Sakura Finetek Japan Co., Ltd., Tokyo) and frozen using powdered dry ice. The frozen samples were stored at −80°C until sectioned and assayed. In the second experiment, the rats were administered intra-gastrically (by gastric intubation) PZ at 200 mg/kg. The rats were immediately decapitated at 1, 2, 3, 4, 6, 12, 24, and 36 h after application of PZ (n = 5 at each time point) and the stomachs were sampled as described above. The Wakayama Medical College Animal Care and Use Committee approved all animal manipulations.

Estimation of gastric mucosal lesions

The stomach was opened along the greater curvature, gently rinsed with saline, and then pinned open to expose the gastric mucosa. The gross appearance of the gastric mucosa was recorded by digital camera (C-7070; Olympus, Tokyo). Mucosal lesions were assessed with the aid of anatomical mapping and tracing software, Neurolucida® with NeuroExplorer™ Ver 5.05.4 (MicroBright Field, Inc., Williston, VT, USA). In short, the digitized images were transferred to a Dell personal computer, and the border of the lesions and the total surface area of the gastric mucosa were traced on a computer by a single observer who was unaware of the treatments. The injured area per total mucosal surface area was calculated.

Pharmacological treatment with SnMP

SnMP (BIOMOL Research Labs., Inc., Plymouth Meeting, PA, USA), an HO-1 inhibitor, was dissolved in 100% ethanol and 10-fold diluted in 7% $NaHCO_3$. The fasted rats received intra-peritoneally vehicle (n = 10) or SnMP (20 μM/kg, n = 10), 60 min before administration of PZ (200 mg/kg).

Group A (n = 5): Vehicle was intra-peritoneally administered; 60 min later, vehicle was again intra-gastrically administered. Group B (n = 5): Vehicle was intra-peritoneally administered; 60 min later, PZ was again intra-gastrically administered. Group C (n = 5): SnMP was intra-peritonealy administered; 60 min later, vehicle was again intra-gastrically administered. Group D (n = 5): SnMP was intra-peritonealy administered; 60 min later, PZ was again intra-gastrically administered.

At 6 h after the application of vehicle or PZ, each rat was administered intragastrically (by gastric intubation) 0.6 N HCl (0.4 ml/100 g). The rats were decapitated and the stomachs were sampled at 2 h after application of HCl.

Real-time RT-PCR

Total RNAs from punched-out gastric tissues were extracted by an RNeasy® Mini Kit (QIAGEN, Tokyo) and digested with RNase free-DNase (QIAGEN). Expression of HO-1 and HSP70 mRNAs was determined by real-time reverse transcriptase (RT)-polymerase chain reaction (PCR). Primers were made using the following sequences based on nucleotides 718 – 979 of rat HO-1 mRNA (22): 5'-AAGAGGCTAAGACCGCC TTC-3' (forward), 5'-GCATAAATTCCCACTGCCAC-3' (reverse); nucleotides 1924 – 2128 of rat HSP70 mRNA (23), 5'-TCTAACACGCTGGCTGAGAA-3' (forward), 5'-CACCCTGAGAGCCAGAAAAG-3' (reverse). As an internal control, we also estimated the expression of rat glyceraldehyde-3 phosphate dehydrogense (GAPDH) mRNA using the following sequences based on nucleotides 904 – 1034 of rat GAPDH mRNA (24): 5'-AGGTTGTCTCCTGTGACTTC-3' (forward), 5'-CTGTTGCTGTAGCCATATTC-3' (reverse). Total RNA (0.1 μg) was converted into cDNA by reverse transcription using random primer p $(dN)_6$ and AMV reverse transcriptase (Roche Diagnostics Corp., Indianapolis, IN, USA) in a total reaction volume of 20 μl. PCR amplification using a LightCycler instrument was

carried out in 20 μl of reaction mixture consisting of LightCycler FastStart DNA Master SYBR Green I (Roche Diagnostics GmbH, Penzberg, Germany), 4.0 mM $MgCl_2$, 0.5 μM of each probe, and 2 μl of template cDNA in a LightCycler capillary. Relative mRNA in each sample was then quantified automatically by reference to the standard curve constructed each time according to the LightCycler software. The levels of mRNA were calculated with reference to external standard curves constructed by plotting the log number of 10-fold serially diluted cDNA samples against the respective threshold cycle by the second derivative maximum method. Each product showed a single band corresponding to the estimated molecular size (HO-1 mRNA, 262 bp; HSP70 mRNA, 205 bp; GAPDH, 309 bp). Expression of mRNA level in each sample was normalized against its GAPDH mRNA level.

Western blotting

The frozen tissues were minced, homogenized in buffer containing 0.01 M Tris-HCl, pH 7.6, 0.15 M NaCl, 1% TritonX-100, and protease inhibitor cocktail (2×10^{-4} M phenylmethanesulfonyl fluoride, 2×10^{-5} M leupeptin, and 1.5×10^{-5} M pepstatin A). The homogenates were centrifuged at $10,000 \times g$ for 15 min at 4°C. Protein concentrations were determined by a Bio-Rad Protein Assay kit (Bio-Rad Laboratories, Inc., Hercules, CA, USA).

The samples were subjected to SDS-polyacrylamide gel (12.5%) electrophoresis and then immunoblotted. After blocking with skim milk, the blots were incubated with antiserum against HO-1 (rabbit polyclonal, SPA-895; Stressgen Biotechnologies Corp., Victoria, Canada) diluted 1:20,000, or antiserum against β-actin (rabbit polyclonal, A5060; Sigma, St. Louis, MO, USA) diluted 1:200 with TBST (0.01 M Tris-HCl, pH 7.6, 0.15 M NaCl, 0.05% Tween 20) containing 1% BSA overnight at 4°C. After washing in TBST, they were incubated with peroxidase-labeled anti-rabbit antibody (NA934; GE Healthcare UK Ltd., Little Chalfont, UK) diluted 1:5,000 in TBST containing 1% BSA for 1 h at 37°C. After washing with TBST, the reaction was visualized by an ECL Western blotting detection kit (GE Healthcare). The signals on the immunoblots were measured by Lumino analyzer LAS-1000 plus (Fuji Film, Tokyo). The protein levels of targets were determined from a relative standard curve constructed by plotting the band densities and normalized by those of β-actin.

In situ hybridization histochemistry

Frozen sections of 6 μm in thickness were cut in a cryostat and thaw-mounted onto silane-coated slides. The probes for detection of HO-1 and HSP70 mRNAs were complementary to nucleotides 276 – 315 of rat HO-1 mRNA (22): GCTCTATCTCCTCTTCCAGGGC CGTATAGATATGGTACAA and to nucleotides 863 – 892 of rat HSP70 mRNA (23): CGATCTCCTTCATCT TGGTCAGCACCATGG. A computer-assisted homology search revealed no identical sequences in any rat genes in the database (GenBank). In situ hybridization histochemistry (ISH) was performed as we previously described (16). The slides were coated with K-5 emulsion (Ilford, Knutsford, UK) diluted 1:2 with water for auto-radiography and then exposed for 6 – 10 weeks at 4°C. Slides were developed in D-19 (Kodak, Rochester, NY, USA), and the sections were counterstained with hematoxylin-eosin for morphological examinations.

Immunohistochemistry

Frozen sections of 6 μm in thickness were cut in a cryostat and thaw-mounted onto silane-coated slides. For double fluorescence immunohistochemistry, sections were incubated simultaneously with the primary antiserum against HO-1 (rabbit polyclonal, SPA-895; Stressgen) or the primary antiserum against HSP70 (rabbit polyclonal, SPA-760; Stressgen) diluted 1:1,000 and monoclonal antibody against macrophage, ED1 (CD68) (mouse monoclonal; Affinity BioReagents, Inc., Golden, CO, USA) diluted 1:200; monoclonal antibody against α-smooth muscle actin (Boehringer Ingelheim GmnH, Ingelheim, Germany) diluted at 1:50; or monoclonal antibody against H^+/K^+ ATPase (β-subunit) (proton pump) (Affinity BioReagents, Inc.) diluted 1:10,000 with 0.1 M PBS containing 5% normal horse serum and 0.3% Triton X-100 for 48 h at 4°C. After rinsing twice with PBS, sections were incubated with the secondary antibody (biotinylated goat anti-rabbit IgG, Vector Laboratories) diluted 1:200 in PBS for 1 h at 37°C. Finally, they were incubated in 1:100 dilution of Texas-Red avidin D (Vector Laboratories), simultaneously with 1:100 dilution of fluorescein isothiocyanate (FITC)-conjugated goat anti-mouse IgG antibody (Jackson ImmunoResearch Lab., West Groove, PA, USA) in 0.1 M PBS containing 5% normal goat serum and 0.3% Triton X-100 for 1 h at 37°C. Omission of the primary or secondary antibody completely eliminated all immunoreactive staining.

Estimation of apoptosis

The degrees of apoptosis were estimated by counting the number of apoptotic cells identified by TUNEL staining (25) and immunostaining of active caspase-3 (26). The TUNEL method detects apoptosis-associated

DNA fragmentation by labeling of the 3'-OH terminal with digoxigenin nucleotides using terminal deoxynucleotidyl transferase (DeadEnd™ Fluorometric TUNEL system; Promega, Madison, WI, USA). We followed the protocol described in the manufacturer's manual. Active caspase-3 was detected by rabbit anti-active caspase-3 polyclonal antibody (BioVision, Mountain View, CA, USA). Frozen sections of 6 μm in thickness were cut in a cryostat and thaw-mounted onto silane-coated slides. Sections were incubated with 3% H_2O_2 in distilled water for 20 min to quench the endogenous peroxidase activity. After rinsing twice with PBS, they were incubated with the primary antiserum against active caspase-3 diluted 1:1,000 with 0.1 M PBS containing 5% normal goat serum and 0.3% Triton X-100 for 48 h at 4°C. Omission of the primary or secondary antibody completely eliminated all immunoreactive staining. After washing in PBS, they were incubated with the secondary antibody (biotinylated goat anti-rabbit IgG, Vector Laboratories) diluted 1:200 in PBS for 1 h at 37°C. After rinsing twice with PBS, they were incubated with avidin-biotin-HRP complex (ABC Elite kit, Vector Laboratories) for 1 h at 37°C. After washing in 0.05 M Tris-HCl buffer, pH 7.6, immunoreactions were visualized by incubation in 0.05 M Tris-HCl buffer, pH 7.6, containing 0.02% 3,3'-diaminobenzidine tetrahydrochloride (DAB) and 0.005% H_2O_2 for 2 – 5 min. The sections were counter-stained with hematoxylin.

The number of apoptotic cells were semi-quantitatively assessed with the aid of anatomical mapping and tracing software, Neurolucida® with NeuroExplorer™ Ver 5.05.4 (MicroBright Field, Inc., Williston, VT, USA). In short, the digitized images were transferred to a Dell personal computer. The immunopositive cells were plotted and the total area of the gastric mucosa was traced on a computer by a single observer who was unaware of the treatments. The number of immunopositive cells per total mucosal area was calculated.

Data analyses

Statistical analysis was performed by one-way ANOVA followed by Fisher's protected least significant difference test or Student's *t*-test using StatView software (Abacus Concepts, Berkeley, CA, USA).

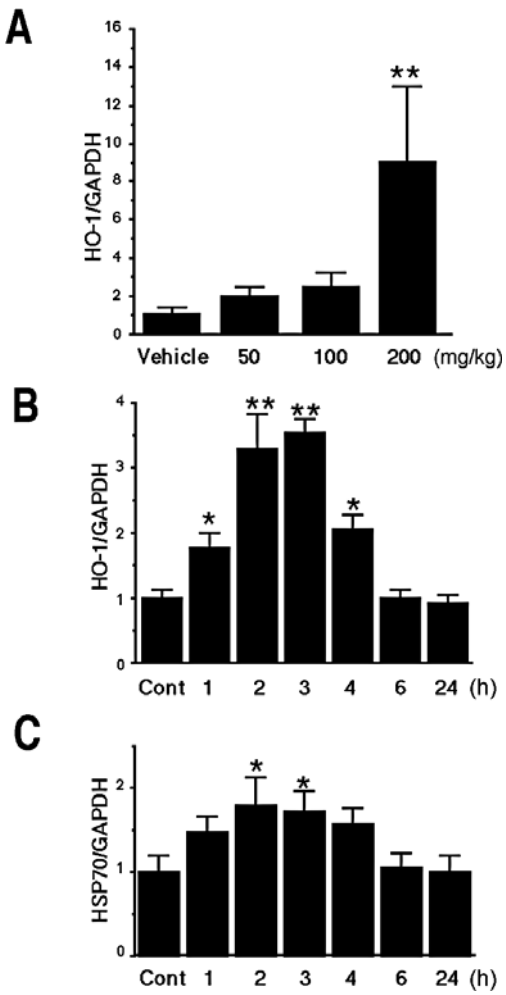

Fig. 1. Expression of HO-1 and HSP70 mRNAs following gastric administration of PZ. A: The rats were intra-gastrically administered PZ at 50, 100, or 200 mg/kg (n = 5, respectively) and the stomachs were sampled at 3 h. B: The rats were intra-gastrically administered PZ at 200 mg/kg and the stomachs were sampled at 1, 2, 3, 4, 6, and 24 h after application of PZ (n = 5 at each time point). Five fasted rats served as controls. Expression of HO-1 and HSP70 mRNAs was determined by RT-PCR. Expression of mRNA level in each sample was normalized against its GAPDH mRNA level. **P*<0.05, ***P*<0.01, compared with the control. The levels of HO-1 mRNA were increased in a dose-dependent manner and a 9-fold increase was observed at 200 mg/kg compared with control levels (A). The levels of HO-1 mRNA were significantly increased at 1 h and maximally increased by 3 – 4-fold at 2 – 3 h compared with control levels (B). The levels of HSP70 mRNA were also maximally increased by 2 – 3-fold at 2 – 3 h compared with control levels (C).

Results

The levels of HO-1 mRNA were increased in a dose-dependent manner, and a 9-fold increase was observed at 200 mg/kg as compared with the control levels (Fig. 1A). The levels of HO-1 mRNA were significantly increased at 1 h and maximally increased by 3 – 4-fold at 2 – 3 h as compared with the control levels. The levels then gradually decreased and returned to the control levels by 6 h (Fig. 1B). The levels of HSP70 mRNA were also maximally increased by 2 – 3-fold at 2 – 3 h as compared with the control levels (Fig. 1C). ISH demonstrated that signals for HO-1 mRNA were observed strongly on the surface mucosal cells and moderately on the scattered cells in the lamina propria and the surrounding submucosa at 3 h (Fig. 2: B and D),

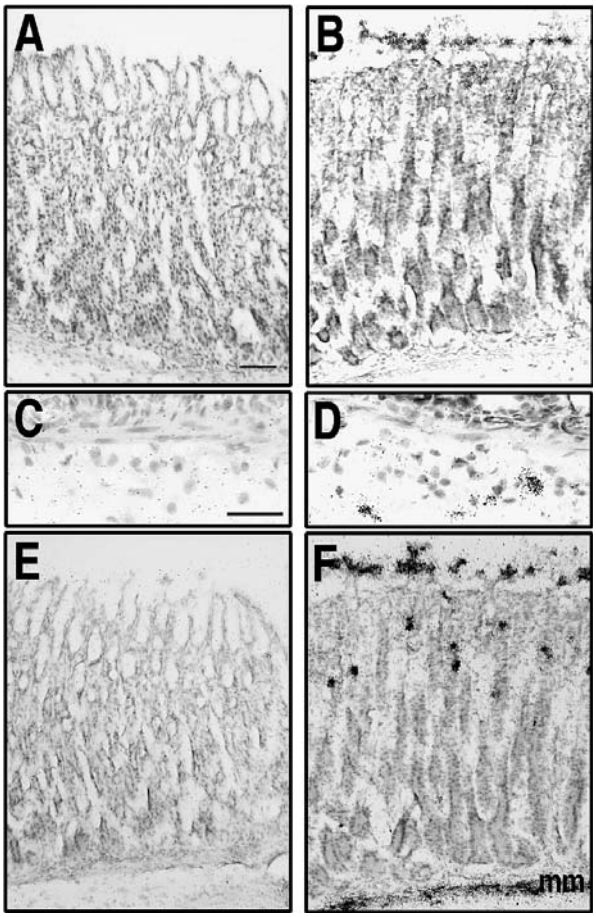

Fig. 2. Localization of HO-1 and HSP70 mRNAs following gastric administration of PZ. Both gastric tissues sampled at 3 h after the application of HCl and the control tissues were fixed in 4% paraformaldehyde in 0.1 M phosphate buffer, pH 7.4. Frozen sections of 6 μm in thickness were cut and used in ISH. A – D: HO-1 mRNA and (E and F) HSP70 mRNA. ISH demonstrated that signals for HO-1 mRNA were observed strongly on the surface mucosal cells and moderately on the scattered cells in the lamina propria and the surrounding submucosa at 3 h (B and D), while these were not detected in the control section (A and C). Signals for HSP70 mRNA were observed strongly on the surface mucosal cells and on the scatted cells and the spindle-like cells in the lamina propria and the muscularis mucosa (mm) (F). In the control section, these signals were not observed (E). Scale bars, 50 μm (A, B, E, and F) and 20 μm (C and E).

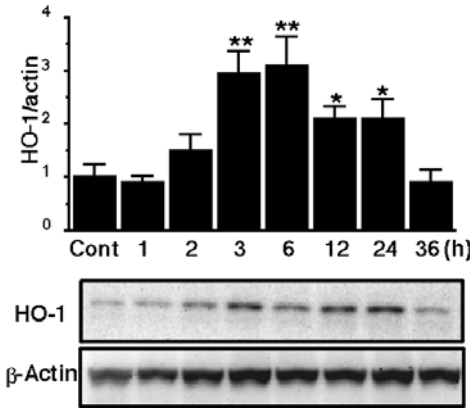

Fig. 3. Expression of immunoreactive HO-1 following gastric administration of PZ. The rats were intra-gastrically administered PZ 200 mg/kg and the stomachs were sampled at 1, 2, 3, 6, 12, 24, and 36 h after application of PZ (n = 5 at each time point). Five fasted rats served as controls. Expression of immunoreactive HO-1 was determined by western blotting. Expression of HO-1 level in each sample was normalized by those of β-actin. Immunoreactive signals for HO-1 were gradually increased, reaching significant levels up to 3-fold higher than the control at 3 – 6 h. They were maintained until 24 h. *P<0.05, **P<0.01, compared with the control.

while these were not detected in the control section (Fig. 2: A and C). Signals for HSP70 mRNA were observed strongly on the surface mucosal cells and on the scattered cells and the spindle-like cells in the lamina propria and the muscularis mucosa (Fig. 2F). In the control section, these signals were not observed (Fig. 2E).

Western blotting showed that immunoreactive signals for HO-1 were gradually increased, reaching significant levels by 3-fold at 3 – 6 h as compared with the control levels. The elevated levels were maintained until 24 h (Fig. 3). HO-1 and HSP70 immunoreactivities were not observed in the control section (Fig. 4: A and B). Clear HO-1– and HSP70-immunoreactive cells were observed at 6 h on the corresponding cells as shown by ISH (Fig. 4: C and D, red color). Omission of the primary antibody completely eliminated the immunoreactivity (not shown). Double fluorescence immunohistochemistry showed that HO-1–immunoreactive cells in the lamina propria and the surrounding submucosa (Fig. 4E, red color) were ED1-positive (Fig. 4E, green color), indicating that they were the macrophages. Double fluorescence immunohistochemistry also showed that HSP70-immunoreactive cells in the muscularis mucosa were α-smooth muscle cells–positive, indicating that they were smooth muscle cells (Fig. 4F).

Two hours after administration of HCl, bloody clots and linear hemorrhages were present on the surface of the damaged mucosa (AGML: acute gastric mucosal lesions). The lesion index in group B (PZ+, SnMP–) was significantly lower as compared with that in group A (PZ–, SnMP–), indicating that pretreatment with PZ prevented the HCl-induced AGML (Fig. 5A, *1). The lesion index in group C (PZ–, SnMP+) was significantly higher than that in group A (PZ–, SnMP–), indicating that inhibition of endogenous HO-1 activity by pretreatment with the HO-1 inhibitor SnMP aggravated the HCl-induced AGML (Fig. 5A, *2). The lesion index in group D (PZ+, SnMP+) was significantly lower as compared with that in the group C (PZ–, SnMP+), indicating that PZ effectively prevented the HCl-induced AGML even though both endogenous and PZ-induced

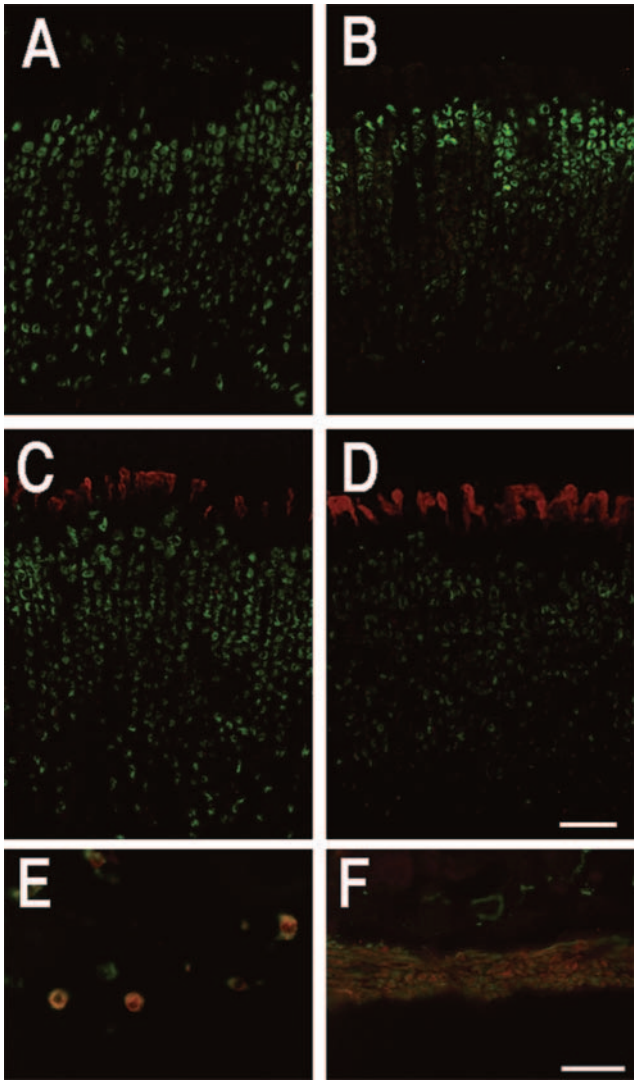

Fig. 4. Localization of immunoreactivities for HO-1 and HSP70 following gastric administration of PZ. Both gastric tissues sampled at 6 h after the application of HCl and the control tissues were fixed in 4% paraformaldehyde in 0.1 M phosphate buffer, pH 7.4. Frozen sections of 6 μm in thickness were cut in a cryostat and double fluorescence immunohistochemistry was performed. HO-1 and HSP70 immunoreactivities were not observed in the control section (A and B, respectively). Clear HO-1 and HSP70 immunoreactive cells (red) were observed at 6 h on the surface mucosal cells (C and D, respectively) as shown by ISH. Immunoreactivities for the proton pump (indicating mucosal parietal cells) are green in color. Scale bars, 50 μm (A – D). HO-1 immunoreactive cells in the submucosa (red) were ED1-positive (green), indicating that they were macrophages (E). HSP70-immunoreactive cells (red) in the muscularis mucosa were α-smooth muscle cells–positive (green), indicating that they were smooth muscle cells (F). Scale bars, 20 μm (E and F).

HO-1 activities were inhibited by SnMP (Fig. 5A, *3). The lesion index in group D (PZ+, SnMP+) was not significantly higher than that in the group B (PZ+, SnMP–) (Fig. 5A, *4). However, the % inhibition in group D (PZ+, SnMP+) was significantly lower than that

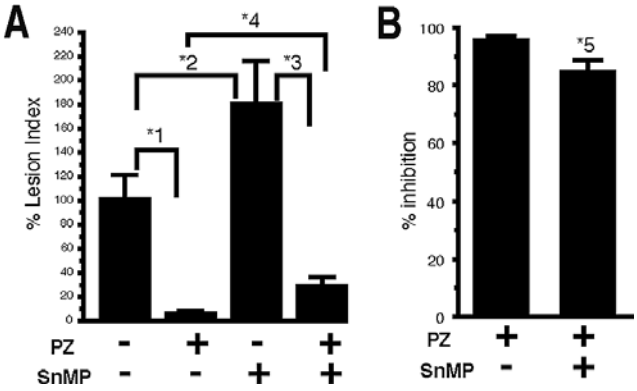

Fig. 5. Evaluation of HCl-induced mucosal lesions following pharmacological treatment with PZ or an HO-1 inhibitor, SnMP. Group A (n = 5): Vehicle was intra-peritoneally administered; 60 min later, vehicle was again intra-gastrically administered. Group B (n = 5): Vehicle was intra-peritoneally administered; 60 min later, PZ was again intra-gastrically administered. Group C (n = 5): SnMP was intra-peritonealy administered; 60 min later, vehicle was again intra-gastrically administered. Group D (n = 5): SnMP was intra-peritonealy administered; 60 min later, PZ was again intra-gastrically administered. At 6 h after the application of vehicle or PZ, each rat was intragastrically administered 0.6 N HCl (0.4 ml/100 g), and the stomachs were sampled at 2 h after application of HCl. The border of each lesion and the total surface area of the gastric mucosa were traced on a computer with the aid of anatomical mapping and tracing software, and the injured area per total mucosal surface area was calculated. Panel A indicates the % lesion index with or without PZ and SnMP. *1, $P<0.001$, vehicle/vehicle (group A) vs. PZ/vehicle (group B); *2, $P<0.05$, vehicle/vehicle (group A) vs. vehicle/SnMP (group C); *3, $P<0.001$, vehicle/SnMP (group C) vs. PZ/SnMP (group D); *4, NS, PZ/vehicle (group B) vs. PZ/SnMP (group D). Panel B indicates the % inhibition of lesion with or without SnMP in the presence of PZ. *5, $P<0.01$.

in the group B (PZ+, SnMP–) (Fig. 5B, *5), suggesting PZ-induced HO-1 was a part of the mucosal protective effects of PZ.

TUNEL staining (Fig. 6A, green color) and immunostaining of active caspase 3 (Fig. 6B, brown color) indicated that apoptotic cells were observed on the surface damaged mucosa. The numbers of TUNEL-positive cells were almost compatible with the lesion index (Fig. 6I). However, the number of apoptotic cells in group B (PZ+, SnMP–) seemed to be smaller, but not significantly so, than that in the group A (PZ–, SnMP–), suggesting that the effect of PZ to prevent the HCl-induced apoptosis of mucosal cells was limited (Fig. 6I, *1). The number of apoptotic cells in group C (PZ–, SnMP+) was significantly higher than that in group A (PZ–, SnMP–), indicating that inhibition of endogenous HO-1 activity by pretreatment with the HO-1 inhibitor increased the HCl-induced apoptosis of mucosal cells (Fig. 6I, *2). The number of apoptotic cells in group D (PZ+, SnMP+) was significantly lower than that in group C (PZ–, SnMP+), indicating that PZ effectively

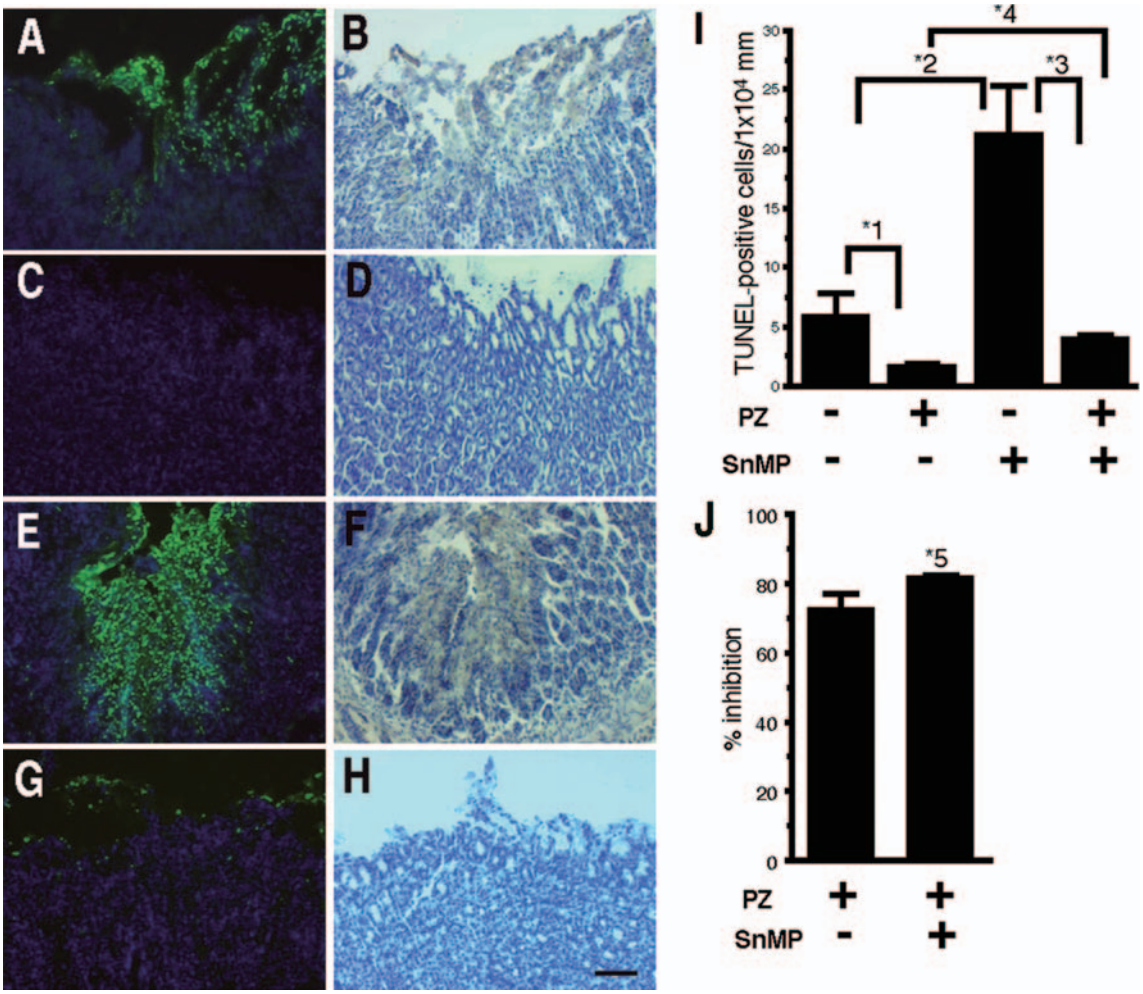

Fig. 6. Evaluation of HCl-induced apoptosis following pharmacological treatment with PZ or SnMP. TUNEL-positive apoptotic cells were colored green and the other cells were counter-stained by DAPI (blue in color) (A, C, E, and G). Immunoreactivities for active caspase 3 were brown in color and counter-stained with hematoxylin (B, D, F, and H). Vehicle/vehicle (A and B), PZ/vehicle (C and D), Vehicle/SnMP (E and F), and PZ/SnMP (G and H). Scale bars, 50 mm. Semi-quantitative analysis of TUNEL-positive cells/area is shown in I. The apoptotic cells were plotted and the total area of the gastric mucosa was traced with the aid of anatomical mapping and tracing software, and the number of TUNEL-positive cells per total mucosal area was calculated. *1, NS, vehicle/vehicle (group A) vs. PZ/vehicle (group B); *2, $P<0.01$, vehicle/vehicle (group A) vs. vehicle/SnMP (group C); *3, $P<0.0001$, vehicle/SnMP (group C) vs. PZ/SnMP (group D); *4, NS, PZ/vehicle (group B) vs. PZ/SnMP (group D). Panel J indicates the % inhibition of apoptosis with or without SnMP in the presence of PZ. *5, NS.

prevented the HCl-induced apoptosis of mucosal cells even though both endogenous and PZ-induced HO-1 activities were inhibited by SnMP (Fig. 6I, *3). The number of apoptotic cells in group D (PZ+, SnMP+) was slightly but not significantly higher than that in group B (PZ+, SnMP–) (Fig. 6I, *4). However, the % inhibition was not significantly changed between group D (PZ+, SnMP+) and group B (PZ+, SnMP–) (Fig. 6J, *5), suggesting that PZ-induced HO-1 did not contribute to the anti-apoptotic effect of PZ.

Discussion

PZ prevents the gastro-intestinal injuries in several experimental models (2 – 9). Several mechanisms of mucosal protection by PZ are considered such as stimulation of mucus production (2), antioxidant activity (6, 7), membrane-stabilizing action (10), and induction of heat shock protein 70 (11). In this study we demonstrated that administration of PZ resulted in the increase of HO-1 mRNA at 2 – 3 h and the increase of immunoreactivities for HO-1 at 3 – 6 h in the stomach. Expression of HSP70 mRNA was also observed at 2 – 3 h in the stomach in accordance with the previous study (11).

HO-1 was strongly induced in the surface gastric mucosal cells and moderately in the gastric macrophages at 3 – 6 h. We also showed that treatment with PZ induced HSP70 strongly in the surface gastric mucosa and, in addition, moderately in the smooth muscle cells in the muscularis mucosa. We previously reported that AGML induced up-regulation of HO-1 in the injured mucosal cells and the macrophages surrounding the lesions (16). In response to AGML, up-regulation of HSP70 was also observed in the injured mucosal cells and the spindle-like cells in the lamina propria and the muscularis mucosa (27). Localization of HO-1 and HSP70 induced by PZ is quite similar to the injury-induced expression, although no obvious mucosal lesions and apoptosis of mucosal cells were observed. These results suggest that PZ can effectively and safely induce cytoprotective HSP70 and HO-1 in the stomach. In the following experiments, we evaluated the protective effects of PZ-induced HO-1 against the HCl-induced AGML and apoptosis of mucosal cells at 6 h after the application of PZ when the PZ-induced expression of HO-1 reached the maximum.

AGML is observed at 15 min after the administration of HCl (16), indicating that heme, a potent pro-oxidant, is released from the pulverized erythrocytes and aggravates the gastric mucosal lesions. In fact, the degrees of mucosal lesions are peaked by 1 h and remain at the same severity until 6 h after the administration of HCl (16). Both endogenous HO-1 and PZ-induced HO-1 are responsible for degrading the pro-oxidative heme and produce equimolar quantities of biliverdin, CO, and free iron (17). Biliverdin is subsequently converted to endogenous anti-oxidative bilirubin via the action of biliverdin reductase. Free iron is promptly sequestered into ferritin, resulting in lowering the pro-oxidant state of the cell. CO improves the microcirculation by vasodilation and inhibition of platelet aggregation (18). Local production of CO will be beneficial since the disturbance of gastric microcirculation is deeply implicated in the pathogenesis of AGML (16). Several lines of studies suggest that HO-1 prevents gastric and colonic damages (14, 15). Metabolites of HO-1 also show protective effects against the gastro-intestinal lesions. For example, systemic application of biliverdin ameliorates experimental colitis (28). Inhalation of CO at a low concentration protects against ishcemia/reperfusion injury in the grafted intestine (29). Therefore, inhibition of HO-1 activity will result in the augmentation of AGML at 2 h after the administration of HCl. It is also expected that the protective effects of PZ will attenuate when PZ-induced HO-1 activity is inhibited.

Treatment with PZ ameliorated the HCl-induced AGML (Fig. 5A, *1), indicating that PZ is an effective anti-ulcer drug in accordance with many previous studies. Inhibition of HO-1 activity by pretreatment with the HO-1 inhibitor SnMP aggravated the HCl-induced AGML (Fig. 5A, *2), indicating that HO-1 has a potential to prevent the irritant-induced AGML. PZ effectively prevented the HCl-induced AGML though both endogenous and PZ-induced HO-1 activities were inhibited by SnMP (Fig. 5A, *3), suggesting that mucosal protection by PZ is attributed to several mechanisms such as stimulation of mucus production (2), antioxidant activity (6, 7), membrane-stabilizing action (10), and induction of heat shock protein (HSP) 70 (11) besides the induction of HO-1. The % inhibition in group D (PZ+, SnMP+) was significantly lower as compared with that in group B (PZ+, SnMP–) (Fig. 5B, *5), suggesting that PZ-induced HO-1 was a part of the mucosal protective effects of PZ.

The numbers of TUNEL-positive cells seemed to be almost compatible with the lesion index. Macroscopic gastric mucosal damages are associated with both apoptosis and necrosis of mucosal cells. It is reported that the short-term treatment (1 h) with high concentrations of various gastric irritants induces the necrosis of mucosal cells, while the long-term treatment (16 h) with low concentrations of irritants induces the apoptosis of mucosal cells (30). In this study, observations were performed at 2 h following application of HCl, suggesting that necrosis but not apoptosis of mucosal cells might be the major pathology, although apoptosis was identified by TUNEL staining and immunostaining of active caspase 3. In fact, treatment with PZ did not significantly reduce the HCl-induced mucosal apoptosis (Fig. 6I, *1), suggesting that the effect of PZ to prevent the HCl-induced apoptosis of mucosal cells was limited. On the contrary, inhibition of endogenous HO-1 by treatment with SnMP increased the number of apoptotic mucosal cells (Fig. 6A, *2), indicating that HO-1 has a potential to prevent the irritant-induced apoptosis of mucosal cells. When both endogenous and PZ-induced activities of HO-1 were inhibited by SnMP, PZ prevented the apoptosis of mucosal cells (Fig. 6I, *3), suggesting that PZ prevents the HCl-induced apoptosis independently of HO-1. The % inhibition of apoptosis was not significantly changed between group D (PZ+, SnMP+) and group B (PZ+, SnMP–) (Fig. 6J, *5), suggesting that PZ-induced HO-1 do not contribute to the anti-apoptotic effect of PZ. These complex results may depend on the coexistence of necrosis and apoptosis in this experimental procedure or the limitation of semi-qualitative estimation of apoptosis.

As PZ is a complex of zinc and L-carnosine, the effects of PZ are the combination of each of these chemicals. L-Carnosine but not zinc sulfate prevented

NH_2Cl-evoked gastric epithelial DNA fragmentation (31), while zinc sulfate but not L-carnosine induced HSP70 in cultured gastric mucosal cells and rat gastric mucosa (11). Zinc sulfate increased glutathione synthesis via the ARE (antioxidant response element) – Nrf2 (nuclear factor erythroid 2-related factor) pathway (32). As induction of HO-1 is also under control of the ARE–Nrf2 pathway (17), PZ-induced induction of HO-1 may also depends on this pathway. Several drugs induce HO-1 in various types of cells. Statins induce HO-1 in vascular smooth muscle cells, endothelial cells, and macrophages (33). Proton pump inhibitors (PPI) also induce HO-1 in endothelial and gastric epithelial cells (34). However, treatment with gastric acid–suppressing agents such as PPI and H_2-receptor antagonists reduced the expression of HSP70 in the gastric mucosa and the gastric mucosa was vulnerable to HCl-induced AGML, while co-administration with PZ restored the resistance against HCl-induced AGML (35). Our data indicated that PZ was effective for preventing the irritant-induced AGML by a combination of multiple mechanisms, at least with induction of HO-1 as well as HSP70.

Involvement of exogenous and endogenous prostaglandin in mucosal protection has well known (36, 37). Cross-talks between the HO-1 system and the cyclooxygenase (COX) system have been demonstrated. It is reported that 15-deoxy-δ 12,14-prostaglandin J_2 exerts an anti-inflamatory effect in macrophages through the action of HO-1/CO (38). In endothelial cells, the HO-1 system regulates the expression of COX, thus influencing the generation of prostaglandin E_2 and prostaglandin I_2 (39). However, Arakawa et al. (2) and Kato et al. (3) demonstrated that the protective effects of PZ were independent of the endogenous prostaglandins. In conclusion, HO-1 is effectively and safely induced by PZ in the stomach and functions as a part of the mucosal protective effects of PZ.

Acknowledgement

This work was supported in part by a Grant-in-Aid from the Japan Society for the Promotion of Science (17590600).

References

1 Matsukura T, Tanaka H. Applicability of zinc complex of L-carnosine for medical use. Biochemistry (Moscow). 2000;65: 817–823.
2 Arakawa T, Satoh H, Nakamura A, Nebiki H, Fukuda T, Sakuma H, et al. Effects of zinc L-carnosine on gastric mucosal and cell damage caused by ethanol in rats. Correlation with endogenous prostaglandin E2. Dig Dis Sci. 1990;35:559–566.
3 Kato S, Nishiwaki H, Konaka A, Takeuchi K. Mucosal ulcerogenic action of monochloramine in rat stomachs: effect of polaprezinc and sucralfate. Dig Dis Sci. 1997;42:2156–2163.
4 Seiki M, Ueki S, Tanaka Y, Soeda M, Hori Y, Aita H, et al. [Studies on anti-ulcer effects of a new compound, zinc L-carnosine (Z-103).] Folia Pharmacol Jpn (Nippon Yakurigaku Zasshi). 1990;95:257–269. (text in Japanese with English abstract)
5 Fujii Y, Matsura T, Kai M, Kawasaki H, Yamada K. Protection by polaprezinc, an anti-ulcer drug, against indomethacin-induced apoptosis in rat gastric mucosal cells. Jpn J Pharmacol. 2000;84:63–70.
6 Yoshikawa T, Naito Y, Tanigawa T, Yoneta T, Kondo M. The antioxidant properties of a novel zinc-carnosine chelate compound, *N*-(3-aminopropionyl)-L-histidinato zinc. Biochim Biophys Acta. 1991;1115:15–22.
7 Yoshikawa T, Naito Y, Tanigawa T, Yoneta T, Yasuda M, Ueda S, et al. Effect of zinc-carnosine chelate compound (Z-103), a novel antioxidant, on acute gastric mucosal injury induced by ischemia-reperfusion in rats. Free Radic Res Commum. 1991; 14:289–296.
8 Ishihara R, Iishi H, Sakai N, Yano H, Uedo N, Narahara H, et al. Polaprezinc attenuates Helicobactor pylori-associated gastritis in Mongolian gerbils. Helicobacter. 2002;7:384–389.
9 Yoshikawa T, Yamaguchi T, Yoshida N, Yamamoto H, Kitazumi S, Takahashi S, et al. Effect of Z-103 on TNB-induced colitis in rats. Digestion. 1997;58:464–468.
10 Cho CH, Luk CT, Ogle CW. The membrane-stabilizing action of zinc carnosine (Z-103) in stress-induced gastric ulceration in rats. Life Sci. 1991;49:PL189–PL194.
11 Odashima M, Otaka M, Jin M, Konishi N, Sato T, Kato S, et al. Induction of a 72-kDa heat shock protein in cultured rat gastric mucosal cells and rat gastric mucosa by zinc L-carnosine. Dig Dis Sci. 2002;47:2799–2804.
12 Rokutan K. Role of heat shock proteins in gastric mucosal protection. J Gastroenterol Hepatol. 2000;15 Suppl:D12–D19.
13 Tsukimi Y, Okabe S. Recent advances in gastrointestinal pathophysiology: role of heat shock proteins in mucosal defense and ulcer healing. Biol Pharm Bull. 2001;24:1–9.
14 Guo X, Shin VY, Cho CH. Modulation of heme oxygenase in tissue injury and its implication in protection against gastrointestinal diseases. Life Sci. 2001;69:3113–3119.
15 Aburaya M, Tanaka K, Hoshino T, Tsutsumi S, Suzuki K, Makise M, et al. Heme oxygenase-1 protects gastric mucosal cells against non-steroidal anti-inflammatory drugs. J Biol Chem. 2006;281:33422–33432.
16 Ueda K, Ueyama T, Yoshida K, Kimura H, Ito T, Shimizu Y, et al. Adaptive HNE-Nrf2-HO1 pathway against oxidative stress is associated with acute gastric mucosal lesions. Am J Physiol Gastrointest Liver Physiol. 2008;295:G460–G469.
17 Otterbein LE, Choi AM. Heme oxygenase: colors of defense against cellular stress. Am J Physiol Lung Cell Mol Physiol. 2000;279:L1029–L1037.
18 Sammut IA, Foresti R, Clark JE, Exon DJ, Vesely MJ, Sarathchandra P, et al. Carbon monoxide is a major contributor to the regulation of vascular tone in aortas expressing high levels of haeme oxygenase-1. Br J Pharmacol. 1998;125:1437–1444.
19 Gopinathan V, Miller NJ, Milner AD, Rice-Evans CA. Bilirubin and ascorbate antioxidant activity in neonatal plasma. FEBS Lett. 1994;349:197–200.
20 Vile GF, Tyrrell RM. Oxidative stress resulting from ultraviolet A irradiation of human skin fibroblasts leads to a heme

oxygenase-dependent increase in ferritin. J Biol Chem. 1993; 268:14678–14681.
21 Li M, Kim DH, Tsenovoy PL, Peterson SJ, Rezzani R, Rodella LF, et al. Treatment of obese diabetic mice with a heme oxygenase inducer reduces visceral and subcutaneous adiposity, increases adiponectin levels, and improves insulin sensitivity and glucose tolerance. Diabetes. 2008;57:1526–1535.
22 Shibahara S, Müller R, Taguchi H, Yoshida T. Cloning and expression of cDNA for rat heme oxygenase. Proc Natl Acad Sci U S A. 1985;82:7865–7869.
23 Mestril R, Chi SH, Sayen MR, Dillmann WH. Isolation of a novel inducible rat heat-shock protein (HSP70) gene and its expression during ischaemia/hypoxia and heat shock. Biochem J. 1994;298:561–569.
24 Piechaczyk M, Blanchard JM, Marty L, Dani C, Panabieres F, El Sabouty S, et al. Post-transcriptional regulation of glyceraldehyde-3-phosphate-dehydrogenase gene expression in rat tissues. Nucleic Acids Res. 1984;12:6951–6963.
25 Hewitson TD, Bisucci T, Darby IA. Histochemical localization of apoptosis with in situ labeling of fragmented DNA. Methods Mol Biol. 2006;326:227–234.
26 Vaculova A, Zhivotovsky B. Caspases: determination of their activities in apoptotic cells. Methods Enzymol. 2008;442:157–181.
27 Saika M, Ueyama T, Senba E. Expression of immediate early genes, HSP70, and COX-2 mRNAs in rat stomach following ethanol ingestion. Dig Dis Sci. 2000;45:2455–2462.
28 Berberat PO, A-Rahim YI, Yamashita K, Warny MM, Csizmadia E, Robson SC, et al. Heme oxygenase-1-generated biliverdin ameliorates experimental murine colitis. Inflamm Bowel Dis. 2005;11:350–359.
29 Nakao A, Kimizuka K, Stolz DB, Neto JS, Kaizu T, Choi AM, et al. Carbon monoxide inhalation protects rat intestinal grafts from ischemia/reperfusion injury. Am J Pathol. 2003;163:1587–1598.
30 Tomisato W, Tsutsumi S, Rokutan K, Tsuchiya T, Mizushima T. NSAIDs induce both necrosis and apoptosis in guinea pig gastric mucosal cells in primary culture. Am J Physiol Gastrointest Liver Physiol. 2001;281:G1092–G1100.
31 Suzuki H, Mori M, Seto K, Nagahashi S, Kawaguchi C, Morita H, et al. Polaprezinc, a gastroprotective agent: attenuation of monochloramine-evoked gastric DNA fragmentation. J Gastroenterol. 1999;34 Suppl 11:43–46.
32 Ha KN, Chen Y, Cai J, Sternberg P Jr. Increased glutathione synthesis through an ARE-Nrf2-dependent pathway by zinc in the RPE: implication for protection against oxidative stress. Invest Ophthalmol Vis Sci. 2006;47:2709–2715.
33 Gueler F, Park JK, Rong S, Kirsch T, Lindschau C, Zheng W, et al. Statins attenuate ischemia-reperfusion injury by inducing heme oxygenase-1 in infiltrating macrophages. Am J Pathol. 2007;170:1192–1199.
34 Becker JC, Grosser N, Waltke C, Schulz S, Erdmann K, Domschke W, et al. Beyond gastric acid reduction: proton pump inhibitors induce heme oxygenase-1 in gastric and endothelial cells. Biochem Biophys Res Commun. 2006;345:1014–1021.
35 Wada I, Otaka M, Jin M, Odashima M, Komatsu K, Konishi N, et al. Expression of HSP72 in the gastric mucosa is regulated by gastric acid in rats-correlation of HSP72 expression with mucosal protection. Biochem Biophys Res Commun. 2006; 349:611–618.
36 Catalioto RM, Festa C, Triolo A, Altamura M, Maggi CA, Giuliani S. Differential effect of ethanol and hydrogen peroxide on barrier function and prostaglandin E2 release in differentiated Caco-2 cells: selective prevention by growth factors. J Pharm Sci. 2009;98:713–727.
37 Zheng X, Oda H, Harada S, Sugimoto Y, Tai A, Sasaki K, et al. Effect of the oral absorption of benzenesulfonanilide-type cyclooxygenase-1 inhibitors on analgesic action and gastric ulcer formation. J Pharm Sci. 2008;97:5446–5452.
38 Lee TS, Tsai HL, Chau LY. Induction of heme oxygenase-1 expression in murine macrophages is essential for the anti-inflammatory effect of low dose 15-deoxy-Delta 12,14-prostaglandin J2. J Biol Chem. 2003;278:19325–19330.
39 Haider A, Olszanecki R, Gryglewski R, Schwartzman ML, Lianos E, Kappas A, et al. Regulation of cyclooxygenase by the heme-heme oxygenase system in microvessel endothelial cells. J Pharmacol Exp Ther. 2002;300:188–194.